

## Experimental Evidence of Boundary-Induced Symmetries in an Optical System with a Kerr-like Non-linearity.

E. PAMPALONI, P. L. RAMAZZA, S. RESIDORI and F. T. ARECCHI(\*)

*Istituto Nazionale di Ottica - 50125 Firenze, Italy*

(received 29 November 1993; accepted 17 January 1994)

PACS. 42.65 – Nonlinear optics.

PACS. 42.90 – Other topics in optics: optical pattern formation.

**Abstract.** – Boundary-dependent patterns with different symmetries are observed in an optical system containing a Liquid-Crystal-Light-Valve acting as a Kerr-like non-linearity. For a small optical aperture, the observed shapes and time-dependent competition confirm recent theoretical predictions.

Spatial pattern formation in extended systems is a topic of current interest in many areas of physics [1]. In particular, many non-linear optical configurations provide naturally two-dimensional wavefronts within which pattern formation can be studied as the fragmentation of the transverse profile of an input beam [2-5].

A crucial problem of pattern formation is to draw a demarcation line between patterns imposed by the boundary-induced symmetries and patterns imposed by the bulk properties of the non-linear medium [6]. Up to now, two different approaches to the problem of pattern formation in optics have been established, namely, one based on the competition (sequential or simultaneous onset) of the lowest-order modes allowed by the boundary symmetries [7-9], and the other one based on the elementary perturbation of an input plane wave due to the medium non-linearities [10].

Very recently a new approach to the problem has been offered [11], in which, starting from the plane-wave approach, a boundary limitation is imposed on the system without resorting to mode expansion of the optical field but only based on symmetry analysis [12]. In particular, for the case of a Kerr medium with a feedback mirror, it is shown [11] that the solutions carrying the full symmetry of the system bifurcate to solutions with a lower symmetry (corresponding to a subgroup of the full symmetry) when boundary limitations are imposed. Therefore, while with plane-wave illumination, patterns are invariant under translations, reflections and rotations in the transverse plane ( $E_2$  symmetry group), and hence rolls and hexagon patterns can be stable [10,13,14], illumination by a confined Gaussian input beam forces the system to be invariant only under rotations and reflections in the transverse plane ( $O_2$  symmetry group). This provides stable solutions with an overall

---

(\*) Also at Physics Department, University of Florence.

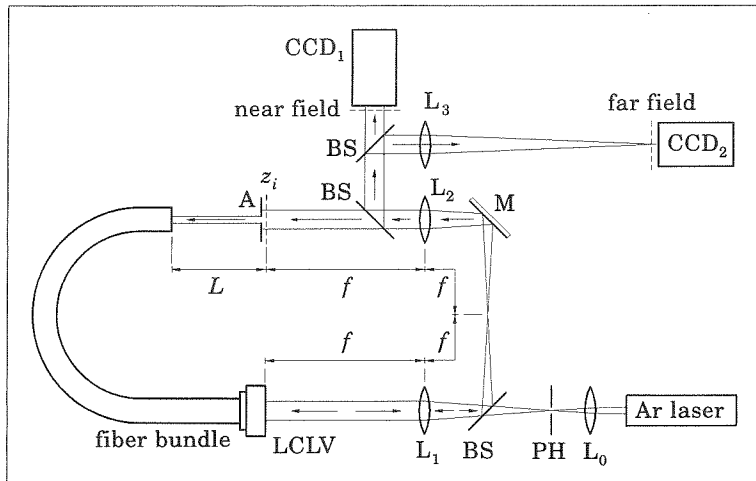


Fig. 1. - Experimental set-up.  $L_{0-3}$  = lenses; M = mirror; BS = beamsplitter; PH = pin hole; A = variable aperture of diameter  $d$ ;  $f$  = focal length of  $L_1$ ,  $L_2$ ;  $L$  = free propagation length. The videocameras  $CCD_1$  and  $CCD_2$  record the patterns in the near-field and in the far-field, respectively.

dihedral symmetry  $D_l$  ( $l$  being an integer) corresponding to a subgroup of  $O_2$  [11]. In this case spatial patterns are characterized by  $l$  axes of symmetry, according to the  $D_l$  group selected by the control parameters.

In this letter we report experimental evidence of this latter scenario, and show a close correspondence with the analytical and numerical results given in ref. [11]. Though preliminary results in this sense have already been given in ref. [15], a complete set of experimental observations is still lacking. Furthermore, in the present experiment we use only phase shift effects, whereas in ref. [15] polarization effects make the system equivalent to a non-linear interferometer. It is worth noticing that in the present configuration our system is completely equivalent to a Kerr slice with a mirror feedback [10,11].

The experimental set-up (fig. 1) is essentially that described in ref. [14]: a collimated Ar laser beam is incident on a Liquid-Crystal-Valve (LCLV) acting as a Kerr-like non-linear medium [16]. The light reflected by the LCLV is fed back through the fibre bundle which is adjusted in such a way that no image rotation is present in the feedback loop. Typically, an a.c. sinusoidal voltage of 15 volt r.m.s. amplitude and 50 kHz frequency is applied to the LCLV.

Since the LC director is parallel to the input beam polarization, we use only phase shift effects, avoiding polarization effects. Thus, the role of the LCLV is to induce on the reflected beam a phase modulation proportional to the intensity of the beam incident on the back of it. The two lenses  $L_1$  and  $L_2$  provide a confocal configuration whereby an image of the front of the LCLV is formed on the plane  $z_i$  (see fig. 1). The distance  $L$  between this plane and the end of the fibre bundle provides a free propagation range where diffraction takes place. The role of diffraction is to convert phase modulation into amplitude modulation so that, by means of the feedback, transverse patterns can arise [10]. The free-propagation distance, which in our experiment is  $L = 100$  cm, determines the wavelength  $\Lambda$  of the patterns [10c]. Precisely, since we deal with a defocusing medium, this is given by  $\Lambda = 2\sqrt{\lambda L/3} = 0.8$  mm where  $\lambda$  is the optical wavelength.

The strength of the non-linearity can be controlled by changing amplitude and frequency

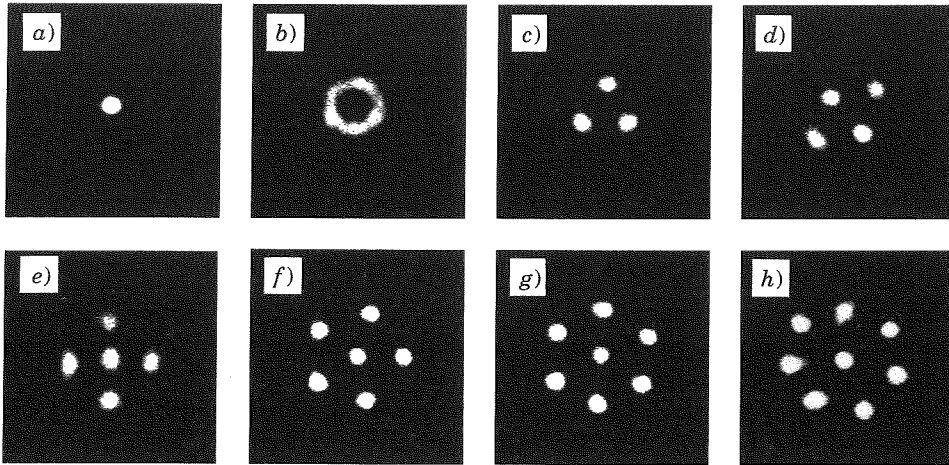


Fig. 2. – Near-field images of the patterns observed for an increasing aperture. *a)* For  $d = 1$  mm only a single spot is allowed by the aperture; *b)* for  $d = 1.1$  mm an annulus goes above threshold; *c)-h)*  $D_l$  symmetries observed, namely, *c)*  $l = 3$  ( $d = 1.2$  mm), *d)*  $l = 2$  ( $d = 1.4$  mm), *e)*  $l = 4$  ( $d = 1.5$  mm), *f)*  $l = 5$  ( $d = 1.7$  mm), *g)*  $l = 6$  ( $d = 1.9$  mm), *h)*  $l = 7$  ( $d = 2.2$  mm).

of the voltage applied to the LCLV, so that large effects can be attained with low intensities  $I$  of the input beam ( $I \approx 20$  mW/cm<sup>2</sup> in our experiment).

In order to check the role of the boundary conditions we insert an aperture on the optical feedback path. Precisely, a variable aperture  $A$  is placed on the image plane  $z_i$  of lens  $L_2$ , providing a confinement of the transverse active region. This way, although the field should be fragmented into hexagons due to the Kerr cubic non-linearity, it is instead forced to fit the aperture area, thus adjusting to the subgroup of the original symmetry allowed by the boundary.

The total diameter of the LCLV is 2 cm, whereas the diameter  $d$  of the diaphragm  $A$  in the feedback loop usually is varied from 1 to 2.2 mm. All the other parameters of the experiment are kept fixed. Starting from  $d = 1$  mm and increasing the aperture in the above range, we observe the subsequent appearance of patterns with symmetry  $D_l$  with  $l$  equal successively to 3, 2, 4, 5, 6, 7. Near-field images of these patterns are shown in fig. 2.

The patterns corresponding to  $D_l$  ( $l = 2, 3, 4, 5, 6, 7$ ) have  $l$  symmetry axes. In most cases this corresponds to  $l$  bright spots arranged at the edges of a polygon of  $l$  sides. The number of spots increases with the aperture, while the separation between spots remains fixed at a value very close to the instability wavelength  $\lambda$ . Only very small adjustments around  $\lambda$  are allowed, due to the fact that we are working very close to the instability threshold. The observed patterns are stationary, but it is worth noticing that they are very

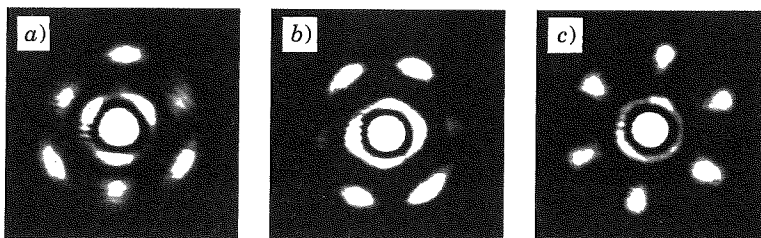


Fig. 3. – Far-field images of patterns with  $D_l$  symmetries: *a)*  $l = 3$ , *b)*  $l = 2$ , *c)*  $l = 6$ .

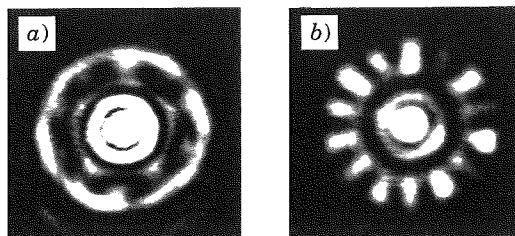


Fig. 4. – Far-field images of patterns with  $D_l$  symmetries: a)  $l = 5$ , b)  $l = 7$ .

sensitive to misalignments so that only a careful adjustment of the optical elements can provide such stable structures.

In fig. 3 we report the far-field images of the patterns with symmetry  $D_l$ ,  $l = 2, 3, 6$ . It can be seen that the far-field maintains a hexagonal-like structure (six spots) even for the cases  $l = 2, 3$  which do not correspond to hexagons in the near field. Figures 3a) and b) can be distinguished from the hexagonal spectrum of fig. 3c) only for some asymmetries in the intensity and spatial arrangement of the peaks. In particular, in the case of  $l = 3$  (fig. 3a)) there are two values of peak intensity spatially alternated, whereas in the case  $l = 2$  one pair of opposite peaks is characterized by a much lower intensity than the other four peaks. An intuitive explanation for the resemblance between the far-fields of these different patterns is that in the case of  $l = 2, 3$  the underlying hexagonal symmetry is not quenched, but it is just prevented from fully displaying in the near-field, as if the aperture picks up only a fraction of an underlying hexagon.

A different situation arises in the cases of  $l = 5$  and  $l = 7$ . In these cases the underlying hexagonal structure is destroyed due to the fact that five or seven spots cannot arrange themselves on a «hexagonal-like» grid. In these cases the far-field images (fig. 4a) and b)) strongly differ from the hexagonal spectrum. The polygonal nature of the pattern appears clearly in the spectrum which is formed by 10 peaks (fig. 4a)) in the case of  $l = 5$  and by 14 peaks (fig. 4b)) in the case of  $l = 7$ .

Besides stationary configurations, we also observe secondary bifurcations which lead to dynamical behaviour of the patterns. Indeed, what we observe is that, changing by small amounts some control parameters (*e.g.* alignment, aperture diameter, frequency and/or amplitude of the voltage applied to the LCLV), in some cases the pattern starts to rotate, in other cases there is an alternation between two patterns corresponding to two successive  $D_l$  groups, and in some other cases the pattern oscillates coherently in time. Though further investigations are needed in order to draw a quantitative bifurcation diagram, qualitatively

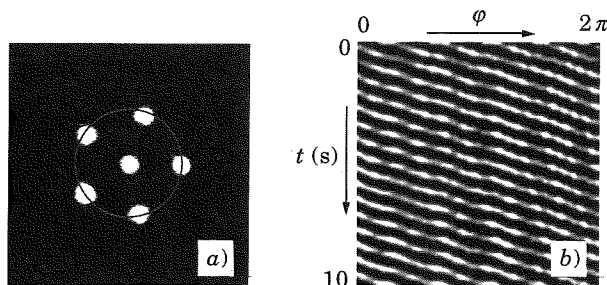


Fig. 5. – a) Rotating pattern with  $D_5$  symmetry; the grey circle corresponds to the data acquisition line. b) Space-time diagram of the rotating pattern: the data acquisition line, as a function of the azimuthal angle  $\varphi$ , is plotted *vs.* time  $t$ .

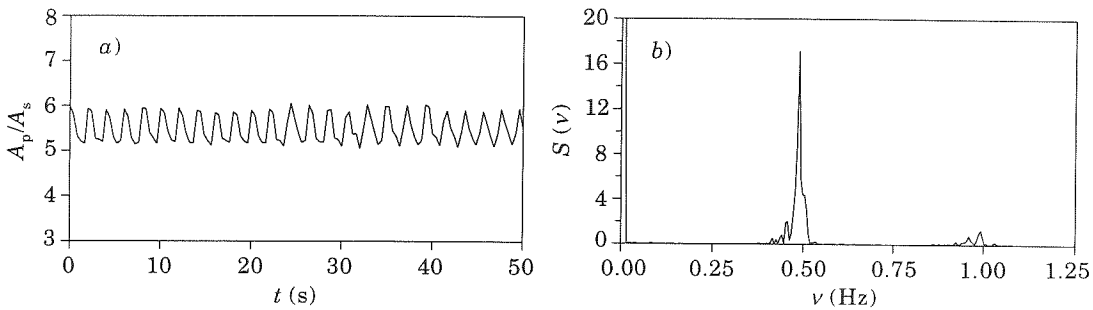


Fig. 6. – Periodic alternation between  $l = 5$  and  $l = 6$  patterns: *a*) time evolution of the measured pattern area  $A_p$ , normalized to the average single-spot area  $A_s$ ; *b*) power spectrum of the signal.

we verify that a small increase of excitation can either bring above threshold more than one solution, thus leading to a periodic alternation between two competing species [3], or introduce a temporal frequency, thus yielding either to a rotation or to an oscillation of the pattern. This scenario is predicted in ref. [1].

In particular, we observe triangular patterns ( $l = 3$ ) coherently oscillating in time,  $l = 3, 5, 6$  patterns rotating and alternations both between  $l = 5, 6$  and  $l = 6, 7$ . By registering in time the light intensity on a circle, as shown in fig. 5*a*) for the case of a pentagon, the rotatory motion of the pattern can be easily visualized on a space-time diagram (fig. 5*b*). Plotting the data on the circle, as a function of the azimuthal angle, for successive time steps, the pattern rotation is transformed into a standing wave in the space-time domain.

Furthermore, by setting the aperture at the diameter  $d = 1.8$  mm, intermediate between the stable operation of the  $l = 5$  and  $l = 6$  patterns, and carefully adjusting the r.m.s. amplitude of the sinusoidal voltage applied to the LCLV, we reach a regime of periodic alternation between the above patterns. Periodic alternation (PA) was first observed in ref. [3] and a dynamical description in terms of a heteroclinic cycle connecting the representative points in phase space was given in ref. [8].

In order to extract a specific indicator for this dynamics, we operate as follows. By looking at the near-field pattern, we thresholded the intensity in order to retain only the bright peaks, and then we sum up, with equal weights, all the pixels whose intensity is above threshold. This technique provides an accurate way for measuring the overall area  $A_p$  occupied by the pattern-forming spots. Normalizing the result to the average area  $A_s$  of a single spot, we have a strong discrimination between the five- and the six-peak pattern. Plotting the normalized pattern area *vs.* time, we obtain a highly periodic time dependence, as shown in fig. 6*a*). Though small environmental fluctuations can slightly affect the measured signal, the period of the alternation remains regular over very long times (our measurements lasted up to 1 hour). Indeed, as shown in fig. 6*b*), the power spectrum of the signal displays clearly the periodic nature of the oscillations.

In conclusion, we have reported the experimental observation of patterns with different symmetries. These symmetries are imposed by the boundary conditions and in particular by the size of the optical aperture. Besides stable attractors corresponding to  $D_l$  symmetries with  $l = 2$  to 7, we have also been able to observe secondary bifurcations toward regimes of pattern rotation and periodic alternation between different symmetries.

\*\*\*

This work has been partially supported by the EEC-Esprit Basic Research action TONICS (Contracts No. 7118).

## REFERENCES

- [1] See, for example: CROSS M. C. and HOHENBERG P. C., *Rev. Mod. Phys.*, **65** (1993) 851.
- [2] AKHMANOV S. A., VORONTSOV M. A. and IVANOV V. YU., *JETP Lett.*, **47** (1988) 707.
- [3] ARECCHI F. T., GIACOMELLI G., RAMAZZA P. L. and RESIDORI S., *Phys. Rev. Lett.*, **65** (1990) 2531.
- [4] KREUZER M., BALZER W. and TSCHUDI T., *Appl. Opt.*, **29** (1990) 579.
- [5] PETROSSIAN A., PINARD M., MAITRE A., COURTOIS J. Y. and GRYNBERG G., *Europhys. Lett.*, **18** (1992) 689.
- [6] ARECCHI F. T., BOCCALETTI S., RAMAZZA P. L. and RESIDORI S., *Phys. Rev. Lett.*, **70** (1993) 2277.
- [7] GREEN C., MINDLIN G. B., D'ANGELO E. J., SOLARI H. G. and TREDICCE J. R., *Phys. Rev. Lett.*, **65** (1990) 3124.
- [8] ARECCHI F. T., BOCCALETTI S., MINDLIN G. B. and PEREZ-GARCIA C., *Phys. Rev. Lett.*, **69** (1992) 3723.
- [9] LUGIATO L. A. and LEFEVER R., *Phys. Rev. Lett.*, **58** (1987) 2209.
- [10] a) FIRTH W. J., *J. Mod. Opt.*, **37** (1990) 151; b) D'ALESSANDRO G. and FIRTH W. J., *Phys. Rev. Lett.*, **66** (1991) 2597; c) D'ALESSANDRO G. and FIRTH W. J., *Phys. Rev. A*, **46** (1992) 537.
- [11] PAPOFF F., D'ALESSANDRO G., OPPO G. L. and FIRTH W. J., *Phys. Rev. A*, **48** (1993) 634.
- [12] GOLUBITSKY M., STEWART I. and SCHAEFFER D., in *Singularities and Groups in Bifurcation Theory II, Applied Mathematical Sciences*, edited by F. JOHN, J. E. MARSDEN and L. SIROVICH, Vol. **69** (Springer-Verlag, New York, N.Y.) 1983.
- [13] MACDONALD R. and EICHLER H. J., *Opt. Commun.*, **89** (1992) 289; TAMBURRINI M., BONAVITA M., WABNITZ S. and SANTAMATO E., *Opt. Lett.*, **18** (1993) 855.
- [14] PAMPALONI E., RESIDORI S. and ARECCHI F. T., *Europhys. Lett.*, **24** (1993) 647.
- [15] ARECCHI F. T., LARICHEV A. V. and VORONTSOV M. A., *Polygon pattern formation in a nonlinear system with a 2D feedback*, to appear in *Opt. Commun.*, **105**, no. 5 (1994).
- [16] AKHMANOV S. A., VORONTSOV M. A., IVANOV V. YU., LARICHEV A. V. and ZHELEZNYKH N. I., *J. Opt. Soc. Am. B*, **9** (1992) 78.